

A convergence formula for sound transmission loss of composite laminates based on three different shear deformation theories

Zhihao Zhang, Renchuan Ye*, Ming Ji, and Guoliang Zhu

Ocean College, Jiangsu University of Science and Technology, Zhenjiang 212003, P.R. China

Received 19 September 2024, Accepted 17 January 2025

Abstract – The Classical Plate Theory (CPT), First-order Shear Deformation Theory (FSDT), and Third-order Shear Deformation Theory (TSDT) have been widely applied in analyzing the Sound Transmission Loss (STL) of composite laminates. However, there are no accurate criteria or formulas to determine the convergence criterion in the process of sound transmission loss analysis. The current method for determining convergence is based on assessing a few typical frequencies to judge convergence across the entire frequency range, resulting in inaccuracies in the high-frequency region and wasting significant computational resources. To address this issue, this paper proposes a new convergence criterion and formula based on CPT, FSDT, and TSDT. These formulas provide a precise framework for determining the optimal number of modes required for convergence, ensuring computational efficiency and accuracy in STL calculations for composite laminates across all frequency ranges.

Keywords: Sound transmission loss, Composite laminates, Convergence criterion

1 Introduction

Currently, scholars have conducted extensive research on the sound transmission loss (STL) of composite laminated plates, and reliable calculation methods for STL based on CPT, FSDT, TSDT, HSDT, and Biot theory have been developed. However, the convergence criteria and calculation formulas for the STL of composite laminates are not yet mature. Relying solely on experience or rough judgments can easily lead to poor accuracy in the results of the high-frequency range of STL.

When the thickness of a plate is less than 1/20 of the wavelength of the deformation mode, the plate can be treated as a thin plate structure. In thin plate analysis, the effects of shear and rotation are neglected in the equations of motion. This is referred to as the Classical Plate Theory. Craven and Gibbs [1, 2] applied CPT to simulate the propagation of sound waves generated at the connection between any structure attached to the plate, demonstrating the accuracy of their results through comparison with previous literature. Lee and Ih [3] utilized CPT to study the STL of finite large single-layer partitions, investigating differences between overall STL and non-resonant STL.

CPT can provide accurate results in the low-frequency range; however, its accuracy diminishes in the high-frequency range. Therefore, the equations should be adjusted using the first-order shear deformation theory in order to consider the impact of shear deformation, yielding more precise results. Shen [4] established a theoretical model for the STL of orthogonally reinforced composite laminates using FSDT. They solved the vibroacoustic governing equations through the spatial harmonic expansion method, providing a basis for further acoustic optimization. Ye [5] simulated the top and bottom plates of composite sandwich panels with a core using FSDT. A linear displacement model was used to analyze the transverse and in-plane displacements of the soft-core layer, examining the transmission loss of vibration and sound in softcore sandwich panels. Based on FSDT, Hu [6] proposed a semi-analytical model for analyzing the STL of functionally graded material plates under thermal loading. The model investigates the impact of material parameters, boundary conditions, and other factors on STL. Fu [7], using FSDT, established an STL model for doublelayer reinforced composite laminates. This model considered the excitation force of plane sound waves and employed the principle of virtual work for an analytical solution, analyzing the influence of geometric parameters on STL. Chandra [8], employing FSDT, analyzed the vibration and STL characteristics of functionally

*Corresponding author: src@just.edu.cn

graded material plates, studying different loads and incident sound waves to analyze their variations. Kim [9] developed a free vibration theoretical model for composite laminates and sandwich panels, using FSDT to establish a mixed variational principle. Their method's accuracy was validated through comparison with previous literature. Chen [10] conducted research on four-edge simply supported functionally graded material sandwich panels based on FSDT. Through numerical comparisons and analysis, the study investigated the characteristics of free vibration and STL, investigating how various parameters impact the fundamental frequency and sound insulation capabilities.

For moderately thick plates or laminates, the influence of transverse shear deformation is significant. The third-order shear deformation theory can better meet the accuracy requirements and provide a better description of shear deformation and shear stress distribution along the thickness direction of the plate. Shi [11] introduced an improved TSDT for analyzing the vibroacoustic problems of shear-flexible plates. It derived consistent variational governing equations and appropriate boundary conditions, which can easily be applied to static and dynamic analyses of laminates. Amabili [12] studied the nonlinear forced vibration of composite laminates using both FSDT and TSDT. It compared response curves calculated using different theories and conducted a thorough analysis of the results. Danesh [13] analyzed the STL of functionally graded material plates under plane wave excitation and external voltage. By combining TSDT with the Hamiltonian principle, it obtained the vibroacoustic governing equation of the plate and solved it analytically to obtain STL curves. Saffari [14] investigated the STL of porous functionally graded materials (PFGM) using TSDT, considering three models with non-uniform core porosity distribution, and assessed the effects of temperature changes on STL. Muc and Flis [15] analyzed the free vibration characteristics of porous functionally graded plates using TSDT and the Ritz method. Vinyas [16], combining TSDT with finite elements, analyzed the vibration frequency response of annular plates. An analytical approach based on TSDT was used by Gunasekaran [17] to analyze the vibroacoustic response of plates made of functionally graded graphene-reinforced composite material. It considered the influence of edge loads on free vibration modes and analyzed resonance amplitudes.

For the analysis of STL in thick plates, it's necessary to consider the higher-order shear deformation theory (HSDT). A simplified approach for solving the free vibration of functionally graded plates using HSDT was introduced by Belabed [18]. The lateral displacement is divided into bending, shearing, and stretching components, significantly reducing the workload of theoretical analysis by reducing the number of unknowns. Mantari [19], based on HSDT, proposed a heartwood composite laminate theory, explaining the approximate parabolic distribution of transverse shear strains with

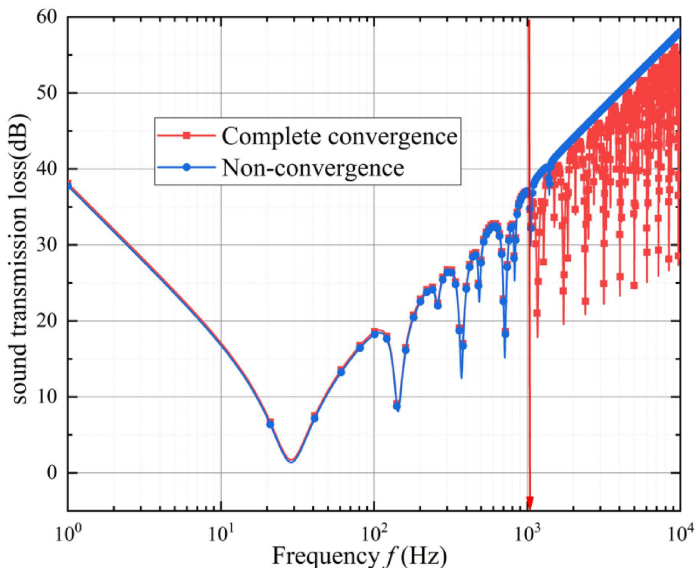


Figure 1. Analysis of the effect of convergence or not on STL.

boundary conditions and analyzing static and dynamic results of different thickness plate shells. Zhang [20, 21] proposed a method considering structural stiffness and strength constraints that significantly improved the sound insulation performance of composite laminates while reducing the mass of the viscoelastic damping layer. Using HSDT, Xu [22] investigated the characteristics of STL in nanocomposite plates reinforced with porous graphene that are functionally graded. They simplified the analysis model and investigated sound radiation and transmission. Naves [23–25] proposed a new HSDT with parabolic variation by expanding the in-plane displacement using sine and hyperbolic functions.

Berryman [26] compared experimental measurements with Biot's theory for composite materials and conducted an analysis of parameters like porosity. Bolton [27] and others used Biot's theory to analyze the propagation of sound waves in porous elastic materials. They derived analytical solutions to calculate the STL of polyurethane foam boards. Ye [28] and Tian [29] studied the sound transmission loss of sandwich plate based on high order shear deformation.

Analyzing the current state of research on STL in composite laminates reveals that the governing equations of motion of these laminates are primarily based on CPT, FSDT, TSDT, HDST, and Biot's theories. However, for laminates, there is currently no reliable convergence criterion and formula for theoretical results of STL. The current approach to determining convergence mainly involves analyzing a few typical frequencies and then estimating the convergence for other frequencies. Yet, if the truncation iteration count does not converge during STL calculations, significant loss of STL data in the high-frequency range can occur, leading to inaccurate results, as shown in Figure 1, in the low-frequency range below 1000 Hz, the results are almost coincident, but the results

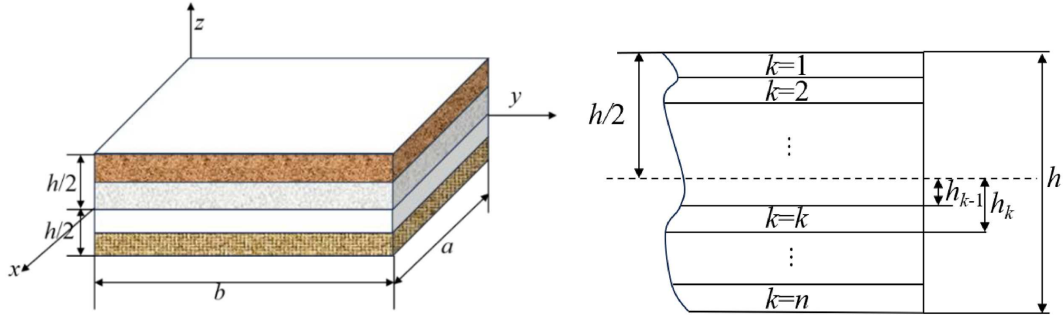


Figure 2. Coordinate system and ply numbering used for laminates.

in the frequency range above 1000 Hz are incorrect. This paper establishes for the first time a convergence criterion and formula for calculating the basic convergent mode numbers of STL in composite laminates. This can be directly used to determine the truncated iteration count for STL across all frequency ranges.

The structure of this paper is as follows. In chapter Two, based on CPT, FSDT, and TSDT, we derive and analyze the theoretical governing equations for STL in composite laminates. Chapter Three presents analysis of the convergence characteristics and parameter influences of laminates and derives the convergence criterion formula for composite laminates. Chapter Four concludes the paper.

2 Theoretical formulation

2.1 Basic assumption

At the current stage, the commonly used thin plate theories are CPT, FSDT, and TSDT. In this section, the accuracy of these theoretical models is verified through calculations, and based on this, the vibration and sound transmission model for laminated plates is derived. According to the CPT, the displacement expression of laminated plates can be written as [30]:

$$\begin{aligned} u_s(x, y, z, t) &= u_{0s}(x, y, t) - z_s \frac{\partial w_0}{\partial x} \\ v_s(x, y, z, t) &= v_{0s}(x, y, t) - z_s \frac{\partial w_0}{\partial y} \\ w_s(x, y, z, t) &= w_{0s}(x, y, t) \end{aligned} \quad (1)$$

where, (u_{0s}, v_{0s}, w_{0s}) is the displacement of laminated along the coordinate axes on the x - y - z plane.

According to the FSDT, the displacement function expression of laminated plates can be written as [30]:

$$\begin{aligned} u_s(x, y, z, t) &= u_{0s}(x, y, t) + z\varphi_x(x, y, t) \\ v_s(x, y, z, t) &= v_{0s}(x, y, t) + z\varphi_y(x, y, t) \\ w_s(x, y, z, t) &= w_{0s}(x, y, t) \end{aligned} \quad (2)$$

where $\varphi_x = \frac{\partial u}{\partial z}$, $\varphi_y = \frac{\partial v}{\partial z}$.

According to the TSDT, the displacement function expression of laminated plates can be written as [30]:

$$\begin{aligned} u_s(x, y, z, t) &= u_{0s}(x, y, t) + z\phi_x(x, y, t) \\ &\quad - \frac{4}{3h^2}z^3 \left(\phi_x + \frac{\partial w_0}{\partial x} \right) \\ v_s(x, y, z, t) &= v_{0s}(x, y, t) + z\phi_y(x, y, t) \\ &\quad - \frac{4}{3h^2}z^3 \left(\phi_y + \frac{\partial w_0}{\partial y} \right) \\ w_s(x, y, z, t) &= w_{0s}(x, y, t). \end{aligned} \quad (3)$$

2.2 Constitutive equation

Assuming that the coordinate system shown in Figure 2 is used, with n orthogonal anisotropic layers, where each layer has an elastic symmetry plane parallel to the x - y plane, we can express the constitutive equation of the layer for a rectangular plate of total thickness h as:

$$\begin{Bmatrix} \sigma_x \\ \sigma_y \\ \sigma_{xy} \\ \sigma_{yz} \\ \sigma_{xz} \end{Bmatrix} = \begin{bmatrix} Q_{11} & Q_{12} & 0 & 0 & 0 \\ Q_{12} & Q_{22} & 0 & 0 & 0 \\ 0 & 0 & Q_{66} & 0 & 0 \\ 0 & 0 & 0 & Q_{44} & 0 \\ 0 & 0 & 0 & 0 & Q_{55} \end{bmatrix} \begin{Bmatrix} \varepsilon_x \\ \varepsilon_y \\ \gamma_{xy} \\ \gamma_{yz} \\ \gamma_{xz} \end{Bmatrix} \quad (4)$$

where, Q_{ij} is the material parameters for each layer:

$$\begin{aligned} Q_{11} &= \frac{E_1}{1 - \nu_{12}\nu_{21}}, & Q_{12} &= \frac{\nu_{12}E_2}{1 - \nu_{12}\nu_{21}} = \frac{\nu_{21}E_1}{1 - \nu_{12}\nu_{21}} \\ Q_{22} &= \frac{E_2}{1 - \nu_{12}\nu_{21}}, & Q_{66} &= G_{12}. \end{aligned} \quad (5)$$

As laminated plates are composed of several orthogonal anisotropic layers, and the material axes of each layer can have any orientation with respect to the laminated plate coordinates, the constitutive equation for each layer must be transformed into the laminated plate coordinates (x, y, z) . The stress-strain relationships in the k layer of

Table 1. Intrinsic frequency results for analytical and numerical solutions.

Mode number (m, n)	CPT (Hz)	FSDT (Hz)	TSDT (Hz)	FEM solution (Hz)	Modal shape
(1, 1)	28.74	28.74	28.74	28.74	
(1, 2)	71.86	71.82	71.85	71.84	
(1, 3)	143.69	143.56	143.68	143.76	
(1, 4)	244.23	243.86	244.20	244.95	
(1, 5)	373.44	372.57	373.36	376.60	
(2, 2)	114.96	114.88	114.95	114.91	
(2, 3)	186.79	186.57	186.76	186.76	
(2, 4)	287.31	286.79	287.26	287.84	
(2, 5)	416.50	415.42	416.40	419.32	
(3, 3)	258.59	258.17	258.55	258.51	
(3, 4)	359.09	358.29	359.01	359.42	
(3, 5)	488.25	486.76	488.10	490.64	
(4, 4)	459.55	458.23	459.42	460.08	
(4, 5)	588.66	586.50	588.45	590.94	
(5, 5)	717.71	714.51	717.40	721.30	

the laminated plate coordinates are given by:

$$\begin{Bmatrix} \sigma_x \\ \sigma_y \\ \sigma_{xy} \\ \sigma_{yz} \\ \sigma_{xz} \end{Bmatrix}^{(k)} = \begin{bmatrix} \bar{Q}_{11} & \bar{Q}_{12} & \bar{Q}_{16} & 0 & 0 \\ \bar{Q}_{12} & \bar{Q}_{22} & \bar{Q}_{26} & 0 & 0 \\ \bar{Q}_{16} & \bar{Q}_{26} & \bar{Q}_{66} & 0 & 0 \\ 0 & 0 & 0 & \bar{Q}_{44} & \bar{Q}_{45} \\ 0 & 0 & 0 & \bar{Q}_{45} & \bar{Q}_{55} \end{bmatrix}^{(k)} \begin{Bmatrix} \varepsilon_x \\ \varepsilon_y \\ \gamma_{xy} \\ \gamma_{yz} \\ \gamma_{xz} \end{Bmatrix}. \quad (6)$$

The transformed material parameter \bar{Q}_{ij} is given by:

$$\begin{aligned} \bar{Q}_{11} &= Q_{11}\cos^4\theta + 2(Q_{12} + 2Q_{66})\sin^2\theta\cos^2\theta + Q_{22}\sin^4\theta \\ \bar{Q}_{12} &= (Q_{11} + Q_{22} - 4Q_{66})\sin^2\theta\cos^2\theta \\ &\quad + Q_{12}(\sin^4\theta + \cos^4\theta) \\ \bar{Q}_{22} &= Q_{11}\sin^4\theta + 2(Q_{12} + 2Q_{66})\sin^2\theta\cos^2\theta + Q_{22}\cos^4\theta \end{aligned}$$

$$\begin{aligned}
\bar{Q}_{16} &= (Q_{11} - Q_{12} - 2Q_{66}) \sin \theta \cos^3 \theta \\
&\quad + (Q_{12} - Q_{22} + 2Q_{66}) \sin^3 \theta \cos \theta \\
\bar{Q}_{26} &= (Q_{11} - Q_{12} - 2Q_{66}) \sin^3 \theta \cos \theta \\
&\quad + (Q_{12} - Q_{22} + 2Q_{66}) \sin \theta \cos^3 \theta \\
\bar{Q}_{66} &= (Q_{11} + Q_{22} - 2Q_{12} - 2Q_{66}) \sin^2 \theta \cos^2 \theta \\
&\quad + Q_{66} (\sin^4 \theta + \cos^4 \theta)
\end{aligned} \tag{7}$$

where, the fiber orientation angle θ represents the angle between the fiber direction of each individual layer and the x -axis.

Assuming that the length and width of the laminated plate are a and b , respectively, the displacement field of the four-ended simply supported plate can be expressed as:

$$\begin{aligned}
\left. \begin{aligned} u(x, y, t) &= \sum_{m=1}^{\infty} \sum_{n=1}^{\infty} U_{mn} \cos \alpha x \sin \beta y \\ \nu(x, y, t) &= \sum_{m=1}^{\infty} \sum_{n=1}^{\infty} V_{mn} \sin \alpha x \cos \beta y \end{aligned} \right\} \\
&\text{(antisymmetric cross-ply)} \\
\left. \begin{aligned} u(x, y, t) &= \sum_{m=1}^{\infty} \sum_{n=1}^{\infty} U_{mn} \sin \alpha x \cos \beta y \\ \nu(x, y, t) &= \sum_{m=1}^{\infty} \sum_{n=1}^{\infty} V_{mn} \cos \alpha x \sin \beta y \end{aligned} \right\} \\
&\text{(antisymmetric angle-ply)} \\
w(x, y, t) &= \sum_{m=1}^{\infty} \sum_{n=1}^{\infty} W_{mn} \sin \alpha x \sin \beta y
\end{aligned} \tag{8}$$

where, $i = \sqrt{-1}$, $\alpha = m\pi/a$, $\beta = n\pi/b$.

To verify the accuracy of the three plate theories mentioned above, a study was conducted on the precision of the free vibration solutions for these theories. Table 1 shows the free vibration of simply supported laminated plates in an air medium, calculated using both theoretical methods and finite element numerical methods. This laminated plate has dimensions of 1 m, with a thickness of 0.002 m for each of the four layers. The density is 1400 kg/m³, Young's modulus is 20e9 Gpa, shear modulus is 7.6923e9 Gpa, Poisson's ratio is 0.3, and the layer angles are [0, 90, 90, 0]. In the finite element method, multi-layer shell elements were used for modeling, with 50 elements in both longitudinal and transverse directions. As shown in Table 1, the results obtained by the three thin shell theories are almost identical to those obtained by the finite element method calculation.

2.3 Equations of fluid and sound boundary conditions

As shown in Figure 3, when the sound wave p_i is incident on the layered panel along the x - z plane at an angle θ_i , it generates reflected sound wave p_r and transmitted sound wave p_t . The layers of the layered panel from top to bottom are the first layer to the n th layer. In the figure, h_n and h_{n+1} are the upper and lower surfaces of the n th layer, respectively. The upper and lower sides of the layered panel are both air media. To facilitate modeling and analysis, cylindrical coordinates are also used to represent the STL.

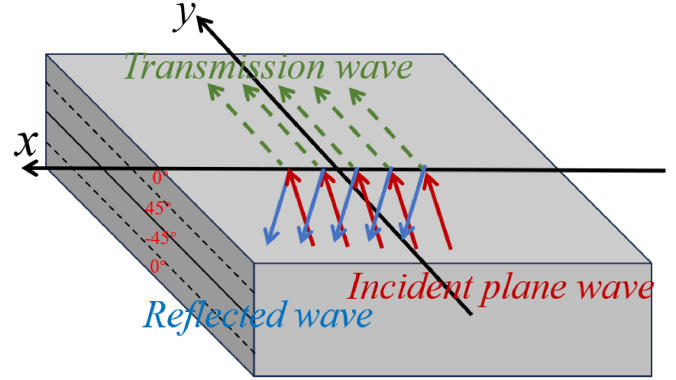


Figure 3. Acoustic wave incidence diagram of laminates [31].

The harmonic incident sound pressure in the plane on the upper surface of the laminate can be described as [6]:

$$p_i(x, y, z) = p_0 e^{j(\omega t - k_x x - k_y y - k_z z)} \tag{9}$$

where, p_0 denotes the incident sound pressure amplitude, ω denotes the acoustic circular frequency, (k_x, k_y, k_z) are the wave number components along the (x, y, z) direction respectively, which can be written as:

$$\begin{cases} k_x = k_0 \sin \varphi \cos \theta \\ k_y = k_0 \sin \varphi \sin \theta \\ k_z = k_0 \cos \varphi \end{cases} \tag{10}$$

where, $k_0 = \omega/c$ denotes the number of waves in the air, and c is the speed of sound.

The reflected sound pressure can be expanded into a double Fourier series [5]:

$$p_r(x, y, t) = \sum_{m=1}^{\infty} \sum_{n=1}^{\infty} R_{mn} \eta_{mn} e^{j(\omega t + k_z z)} \tag{11}$$

where, $\eta_{mn} = \sin \alpha x \sin \beta y$, $\alpha = m\pi/a$, $\beta = n\pi/b$; R_{mn} is the m - n order reflected sound pressure amplitude.

The transmitted sound pressure can be described as:

$$p_t(x, y, t) = \sum_{m=1}^{\infty} \sum_{n=1}^{\infty} T_{mn} \eta_{mn} e^{j(\omega t - k_z z)} \tag{12}$$

where, T_{mn} is the m - n order transmitted sound pressure amplitude.

$$T_{mn} = \frac{j \rho_0 \omega^2 W_{bmn}}{k_z} e^{j \frac{h k_z}{2}}. \tag{13}$$

2.4 The governing equations for composite laminates based on the theories of CPT, FSDT, and TSDT are as follows

Continuing with the study of the acoustic transmission loss for the CPT, the FSDT and the TSDT, and deriving the control equations for the laminated under the three theories, the matrix form of the control equations of motion for the three theories is given below.

The transfer matrix equation for laminates based on CPT [30] is:

See the Equation (14) bottom of the page

The nonzero elements are given in Appendix A.

The transfer matrix equation for laminates based on the FSDT [30] is given by:

$$\left(\begin{bmatrix} S_{11} & S_{12} & 0 & S_{14} & S_{15} \\ S_{12} & S_{22} & 0 & S_{24} & S_{25} \\ 0 & 0 & S_{33} & S_{34} & S_{35} \\ S_{14} & S_{24} & S_{34} & S_{44} & S_{45} \\ S_{15} & S_{25} & S_{35} & S_{45} & S_{55} \end{bmatrix} - \omega^2 \begin{bmatrix} I_0 & 0 & 0 & 0 & 0 \\ 0 & I_0 & 0 & 0 & 0 \\ 0 & 0 & I_0 & 0 & 0 \\ 0 & 0 & 0 & I_2 & 0 \\ 0 & 0 & 0 & 0 & I_2 \end{bmatrix} \right) \begin{Bmatrix} U_{mn} \\ V_{mn} \\ W_{mn} \\ X_{mn} \\ Y_{mn} \end{Bmatrix} = \begin{Bmatrix} 0 \\ 0 \\ P_{mn} \\ 0 \\ 0 \end{Bmatrix}. \quad (15)$$

The nonzero elements are given in Appendix B.

The transfer matrix equation for laminates based on the TSDT [30] is given by:

See the Equation (16) bottom of the page

The nonzero elements are given in Appendix C.

2.5 Validation of sound transmission loss

By applying the Fourier transform to the incident sound pressure, we can obtain the following translation [6]:

$$I_{mn} = \frac{4mn\pi (e^{-jk_x a} \cos m\pi - 1) (e^{-jk_y b} \cos n\pi - 1) p_0}{[(k_x a)^2 - (m\pi)^2] [(k_y b)^2 - (n\pi)^2]}. \quad (17)$$

The sound transmission loss can be expressed as:

$$\text{STL} = 10 \log_{10} \left(\frac{\sum_{m=1}^{\infty} \sum_{n=1}^{\infty} |I_{mn}|^2}{\left(\sum_{m=1}^{\infty} \sum_{n=1}^{\infty} |T_{mn}|^2 \right)} \right). \quad (18)$$

To verify the correctness of the theoretical derivations in this paper, the laminated plate shown in Table 2 is selected as a reference example, and finite element analysis software COMSOL is used for comparative calculations with four-end simply supported boundary conditions. Considering the incident angles along the x -axis and z -axis relative to the plane of the sound waves, the calculation results are shown in Figure 4. The CPT calculation results show slight deviations compared to FSDT and TSDT, which is due to the neglect of layer-wise shear deformation effects in the assumptions of CPT. A comparison with the finite element method shows that the curves roughly overlap, thereby validating the accuracy of the analytical method proposed in this paper.

3 Validation of sound transmission loss and convergence analysis

3.1 Analysis of convergence characteristics of sound transmission loss

The convergence curve of acoustic transmission loss of laminated at 20000 Hz frequency is shown in Figure 5, and the curve exists in three regions: non-convergence region, basic convergence region and complete convergence region, which are defined as follows in this paper:

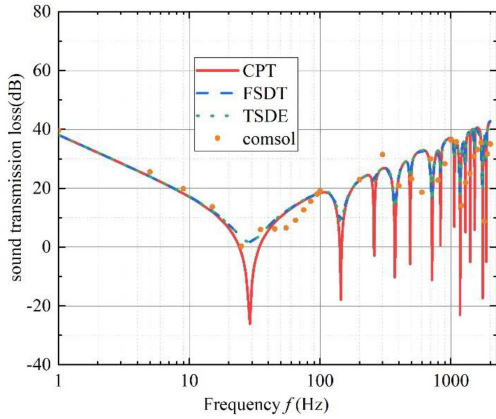
Non-convergence zone (NCz): When the number of modal iterations is less than 41, it can be seen that the error between the acoustic transmission loss value and

$$\left(\begin{bmatrix} s_{11} & s_{12} & s_{13} \\ s_{12} & s_{22} & s_{23} \\ s_{13} & s_{23} & s_{33} \end{bmatrix} - \omega^2 \begin{bmatrix} I_0 & 0 & 0 \\ 0 & I_0 & 0 \\ 0 & 0 & \bar{I}_0 \end{bmatrix} \right) \begin{Bmatrix} U_{mn} \\ V_{mn} \\ W_{mn} \end{Bmatrix} = \begin{Bmatrix} 0 \\ 0 \\ P_{mn} \end{Bmatrix}. \quad (14)$$

$$\left(\begin{bmatrix} S_{11} & S_{12} & S_{13} & S_{14} & S_{15} \\ S_{12} & S_{22} & S_{23} & S_{24} & S_{25} \\ S_{13} & S_{23} & S_{33} & S_{34} & S_{35} \\ S_{14} & S_{24} & S_{34} & S_{44} & S_{45} \\ S_{15} & S_{25} & S_{35} & S_{45} & S_{55} \end{bmatrix} - \omega^2 \begin{bmatrix} m_{11} & 0 & 0 & 0 & 0 \\ 0 & m_{22} & 0 & 0 & 0 \\ 0 & 0 & m_{33} & m_{34} & m_{35} \\ 0 & 0 & m_{34} & m_{44} & 0 \\ 0 & 0 & m_{35} & 0 & m_{55} \end{bmatrix} \right) \begin{Bmatrix} U_{mn} \\ V_{mn} \\ W_{mn} \\ X_{mn} \\ Y_{mn} \end{Bmatrix} = \begin{Bmatrix} 0 \\ 0 \\ p_{mn} \\ 0 \\ 0 \end{Bmatrix}. \quad (16)$$

Table 2. Laminated material parameters.

Symbol	Description	Value	Unit
Physical parameter			
h	Thickness of each layer	0.002	m
a	Length	1	m
b	Width	1	m
n	Layers	4	
Material parameter			
$E_1 = E_2$	Young's modulus	20e9	pa
$G_{12} = G_{13} = G_{23}$	Shear modulus	7.6923e9	pa
μ	Poisson's ratio	0.3	
ρ	Density	1400	kg/m ³
Air parameters			
P_0	Amplitude of incident sound pressure	1	Pa
c	Velocity of sound in air	343	m/s
ρ_0	Air density	1.21	kg/m ³

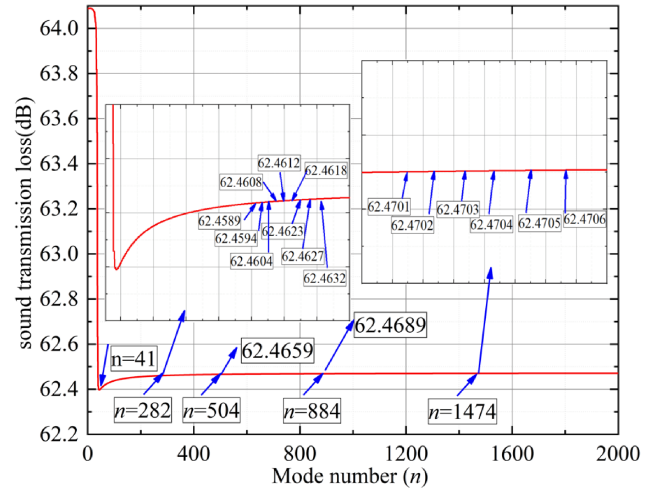
**Figure 4.** Comparison of the results of the analytical solution and the finite element method for acoustic transmission loss.

the value of the acoustic transmission loss in the case of complete convergence is greater than 0.1 dB. The region where it is true is called the non-convergencezone.

Basic convergence zone (BCz): When the number of modal iterations reaches 41 times, it can be seen that the error between the acoustic transmission loss value and the value of acoustic transmission loss in the case of complete convergence is less than 0.1 dB, and this region is called the basic convergence zone.

Complete Convergence Zone (CCz): When the number of modal iterations reaches 1474, it can be seen that the change value of the STL value has been less than 0.0001 dB, and this area is called the complete convergence zone.

Considering the reasonable allocation of computational resources, when the number of modal iterations reaches 41 times, the calculation results of STL of laminated no longer appear to jump or lack precision, so when carrying out the acoustic transmission loss calculation, the modal number adopts the value of the basic convergence zone to fully comply with the requirements of the computational accuracy.

**Figure 5.** Convergence analysis of STL in laminated.

3.2 Influence of medium parameters on convergence

The convergence of the acoustic transmission loss of the laminated at different frequencies is shown in Figure 6, which indicates that the number of iterations of the acoustic transmission loss of the laminated at different frequencies is different, and the number of modal iterations required to reach complete convergence is higher with the higher frequency, and the number of modes in the case of complete convergence is linearly related to the frequency. The analysis of the number of iterations required for convergence at different frequencies shows that the convergence is very fast in the range of 1000 Hz to 80 000 Hz, and the number of iterations required to reach full convergence increases with the increase of frequency and is linearly related to the frequency of the incident acoustic wave as shown in Figure 7, and the number of modes required to reach full convergence is a logarithmic function for different thicknesses as the frequency increases and the number of modes required to achieve full convergence becomes smaller with the increase of thickness, and therefore, the formula for the convergence criterion

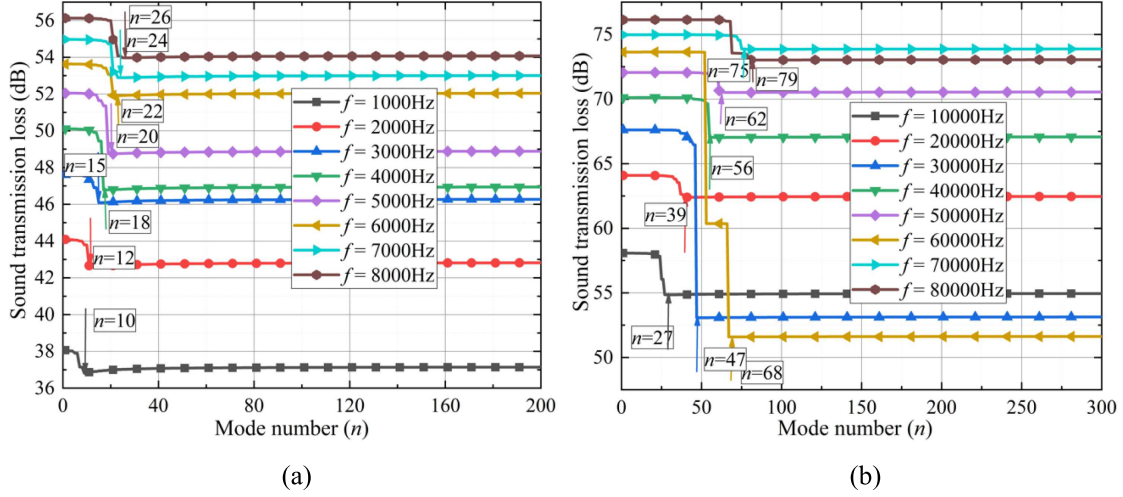


Figure 6. Convergence value of STL of laminated at different frequencies. (a) 1000 Hz ~ 8000 Hz (b) 8000 Hz ~ 80000 Hz.

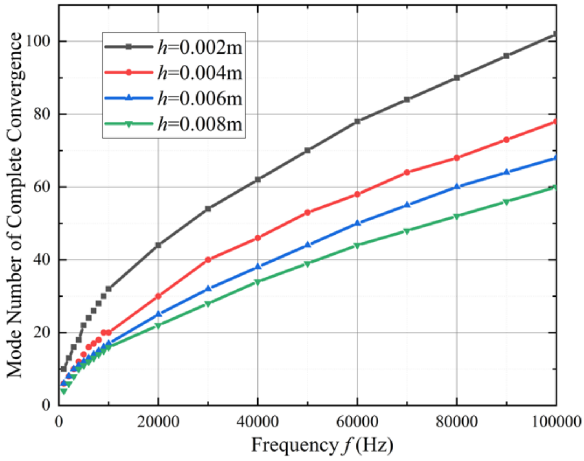


Figure 7. Fully converged modal number versus frequency. can be described as follows:

$$M(f) = k(h)f^{m(h)} \quad f > 0, k(h) > 0, m(h) > 0 \quad (19)$$

where, $M(f)$ is the modulus, $k(h)$, $m(h)$ denotes a coefficient related to the thickness of the laminated and f denotes the frequency of the incident acoustic wave.

In order to establish a generalized convergence criterion for the acoustic transfer loss of laminates, it is necessary to analyze the convergence of some important parameters affecting the acoustic transfer loss of laminates. As shown in Figures 8 and 9, the effects of Young's modulus and shear modulus of the laminated on the convergence of the STL are analyzed respectively, and it can be seen that the Young's modulus and shear modulus of the laminated have no effect on the STL.

The effect of different laminated thicknesses on the convergence of STL is shown in Figure 10, and it can be seen that the convergence of laminated thickness is related to the number of modes, and the number of iterations for complete convergence decreases with the increase of shell thickness and is linearly correlated, and the change is more obvious at 20000 Hz, and in

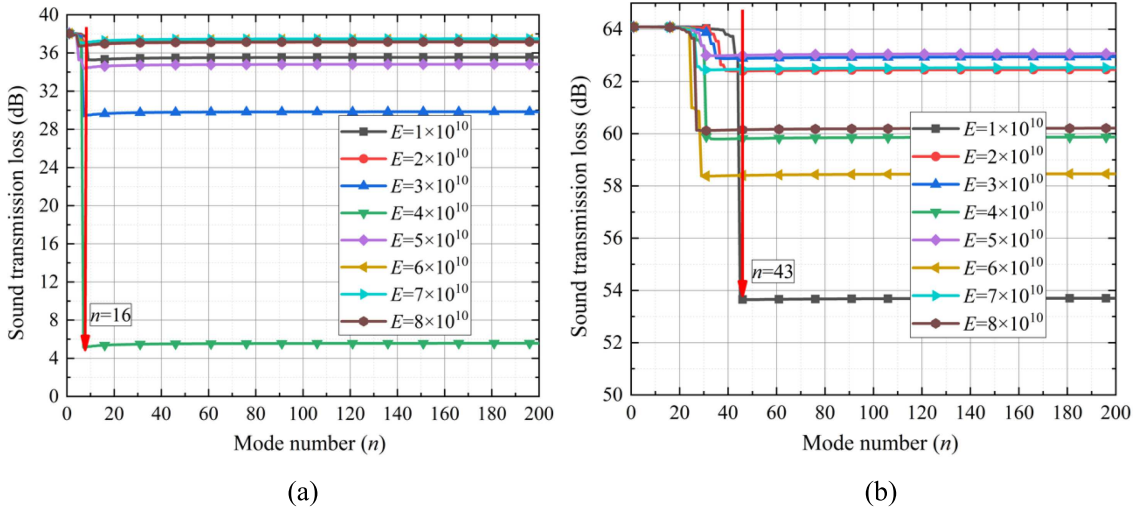


Figure 8. Convergence values of STL for laminates with different Young's modulus (1000 Hz, 20000 Hz). (a) 1000 Hz. (b) 20000 Hz.

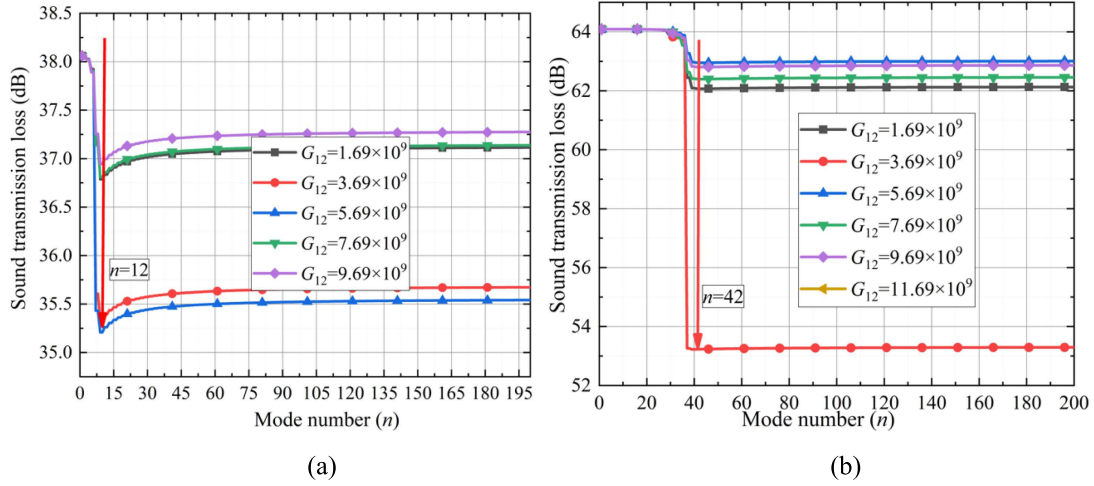


Figure 9. Convergence values of STL for laminates with different shear modulus (1000 Hz, 20000 Hz). (a) 1000 Hz. (b) 20000 Hz.

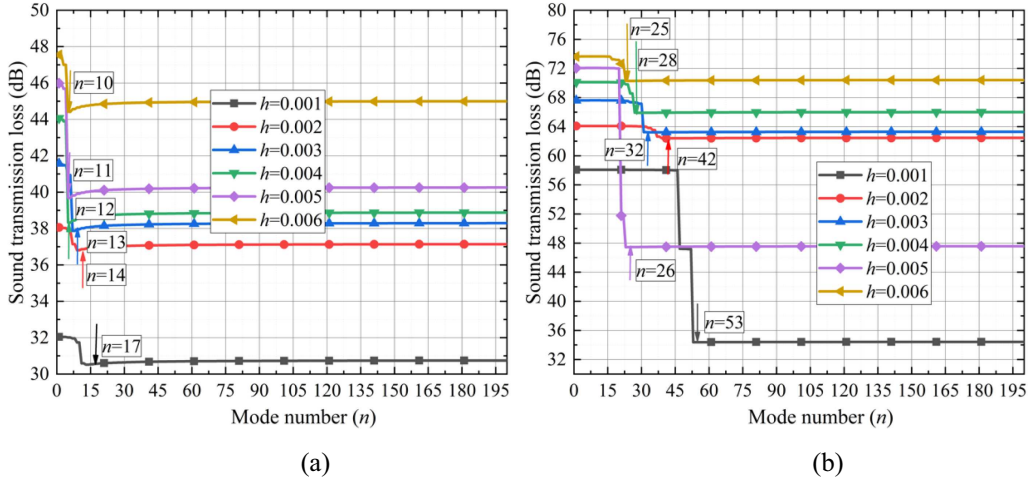


Figure 10. Convergence values of STL for different thicknesses of laminated (1000 Hz, 20000 Hz). (a) 1000 Hz. (b) 20000 Hz.

the laminated thicknesses of 0.001 m, 0.002 m, 0.003 m, respectively, 0.004 m, 0.005 m, 0.006 m, the number of fully converged iterations are 53, 42, 32, 28, 26, 25, respectively, and it can be concluded that the number of iterations and the thickness are in inverse logarithmic function. Meanwhile, in order to verify the correctness of the above conclusions as well as to propose the relevant convergence criterion formula, the relationship between the number of iterations and the thickness at 10000 Hz, 20000 Hz, 30000 Hz and 40000 Hz is calculated, as shown in Figure 11, which shows that the number of iterations and the thickness all exhibit the linear relationship described above, and the convergence criterion formula of the thickness of the laminated is:

$$M(h) = k(f)h^{m(f)} \quad h > 0, k(f) > 0, m(f) < 0 \quad (20)$$

where, $M(h)$ is the number of modes of complete convergence, $k(f), m(f)$ is the correlation coefficient of the incident sound wave.

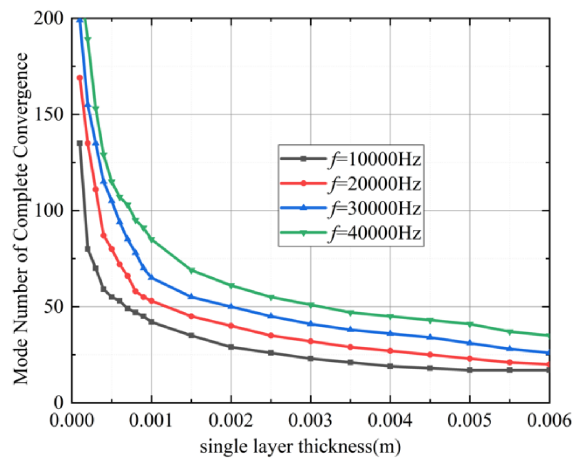


Figure 11. Completely convergent relationship between the number of modes and thickness.

The effect of different laminated edge lengths on the convergence of STL is shown in Figure 12, which shows that

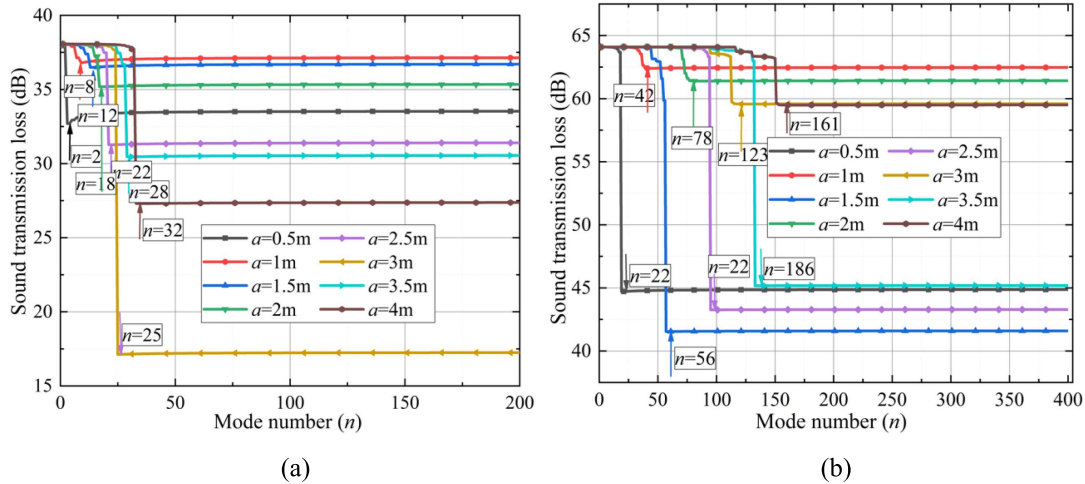


Figure 12. Convergence values of STL for laminates with different edge length (1000 Hz, 20 000 Hz). (a) 1000 Hz. (b) 20 000 Hz.

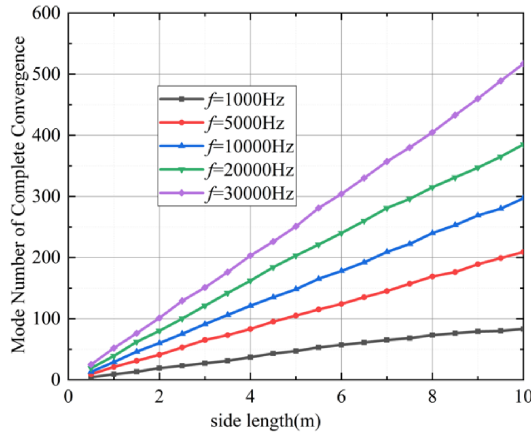


Figure 13. Fully converged modal number versus edge length.

the convergence of laminated edge lengths is related to the number of modes, the number of fully converged iterations increases with the increase of edge lengths, and the number of fully converged iterations is linearly correlated to the laminated edge lengths. At the laminated side lengths of 0.5 m, 1 m, 1.5 m, 2 m, 2.5 m, 3 m, 3.5 m, and 4 m, the number of iterations for complete convergence at 1000 Hz is 2, 8, 12, 18, 22, 25, 28, and 32, respectively, and it can be concluded that the number of iterations required for complete convergence is directly proportional to that of the laminated. In order to verify the correctness of the above conclusion, the comparison curves of modal number and STL at 20 000 Hz with different laminated edge lengths are calculated as shown in Figure 13, and it can be found that the modal number is proportional to the laminated edge length at 20 000 Hz. Therefore, the convergence criterion equation for the laminated edge length is:

$$M(a) = k(f)a + b \quad f > 0, \quad a > 0, \quad k(f) > 0 \quad (21)$$

where, $M(a)$ denotes the number of modes at full convergence, $k(f)$ denotes the frequency correlation

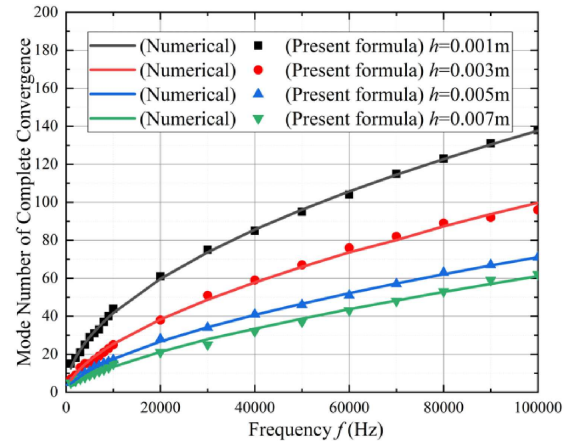


Figure 14. Comparison of present convergence formula and numerical results in different sound wave frequency.

coefficient of the incident acoustic wave on the surface of the laminated, a and b denotes laminated edge length.

3.3 Convergence criteria and formula verification

The relationship between the number of fully convergent modes and the frequency of incident sound wave, the thickness of laminates and the length of laminates can be summarized as follows:

$$\begin{cases} M(f) = k(h)f^{m(h)} & f > 0, \quad k(h) > 0, \quad m(h) > 0 \\ M(h) = k(f)h^{m(f)} & h > 0, \quad k(f) > 0, \quad m(f) < 0 \\ M(a) = k(f)a + b & f > 0, \quad a > 0, \quad k(f) > 0 \end{cases} \quad (22)$$

To further verify the accuracy of the convergence criterion formula, the theoretical and numerical modal numbers of the C -layer laminated (parameters shown in Tab. 2) are shown in Figures 14, 15 respectively. The modal numbers obtained from the convergence formula are completely consistent with those obtained from

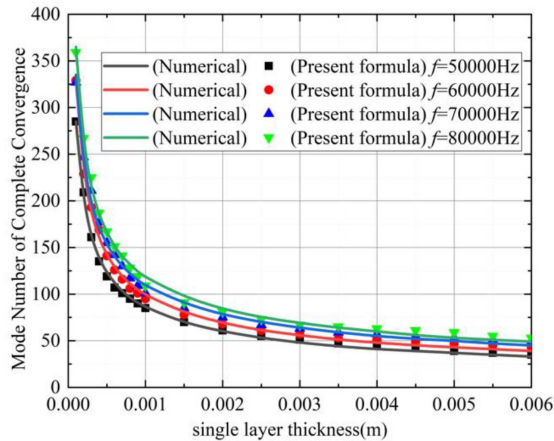


Figure 15. Comparison of present convergence formula and numerical results in different single layer thickness.

numerical calculations for complete convergence, thus once again proving that the convergence formula proposed in this paper has high accuracy.

4 Conclusion

In this paper, an analytical model for STL analysis of laminated structures is derived using three thin plate theories. Based on the CPT, FSDT and TSDT theories, convergence criteria and formulas for the calculation of STL in laminated are established. The following conclusions can be drawn:

- (1) Based on the three theories of CPT, FSDT and TSDT, a new convergence criterion and formula for calculating the STL of laminates are proposed, which can be directly used to determine the truncated iteration of STL in each frequency range.

$$\begin{cases} M(f) = k(h) f^{m(h)} & f > 0, \quad k(h) > 0, \quad m(h) > 0 \\ M(h) = k(f) h^{m(f)} & h > 0, \quad k(f) > 0, \quad m(f) < 0. \\ M(a) = k(f) a + b & f > 0, \quad a > 0, \quad k(f) > 0 \end{cases} \quad (23)$$

- (2) The laminated STL curve has three distinct regions (non-convergence region, basic convergence region and full convergence region). As the frequency increases, the computational resources required to achieve full convergence will significantly increase, and on balance, the basic convergence region can be used.
- (3) The STL convergence curves obtained based on the three theories of CPT, FSDT and TSDT almost overlap; Young's modulus and shear modulus of the laminated have no effect on the STL; the number of iterations required for complete convergence decreases with increasing shell thickness, but increases with increasing length.

Acknowledgments

This study was supported financially by the National Natural Science Foundation of China (Grant nos. 52001145/52271319), the Natural Science Foundation of Jiangsu Province of China (BK20180976).

Conflicts of interest

The authors declare that they have no known competing financial interests or personal relationships that could have appeared to influence the work reported in this paper.

Data availability statement

Data are available on request from the authors.

References

1. P.G. Craven, B.M. Gibbs: Sound transmission and mode. coupling at junctions of thin plates, part I: representation of the problem. *Journal of Sound and Vibration* 77 (1981) 417–427.
2. B.M. Gibbs, P.G. Craven: Sound transmission and mode. coupling at junctions of thin plates, part II: parametric survey. *Journal of Sound and Vibration* 77 (1981) 429–435..
3. J.H. Lee, J.G. Ih: Significance of resonant sound. transmission in finite single partitions. *Journal of Sound & Vibration* 277 (2004) 881–893..
4. C. Shen, F.X. Xin, T.J. Lu: Sound transmission across. composite laminate sandwiches: influence of orthogonal stiffeners and laminate layup. *Composite Structures* 143 (2016) 310–316..
5. R. Ye, A. Tian, Y. Chen, N. Zhao, W. Yang, P. Ren.: Sound transmission characteristics of a composite sandwich plate using multi-layer first-order zigzag theory. *Thin-Walled Structures*. 179 (2022) 109607.
6. Z. Hu, K. Zhou, S. Huang, Y. Chen: Sound transmission. analysis of functionally graded material plates with general boundary conditions in thermal environments. *Applied Acoustics* 174 (2021) 107795..
7. T. Fu, Z. Chen, D. Yu, X. Wang, W. Lu: Sound transmission from. stiffened double laminated composite plates. *Wave Motion* 72 (2017) 331–341..
8. N. Chandra, S. Raja, K.V.N. Gopal: Vibro-acoustic. response and sound transmission loss analysis of functionally graded plates. *Journal of Sound and Vibration* 333 (2014) 5786–5802..
9. J.S. Kim: Free vibration of laminated and sandwich plates using enhanced plate theories. *Journal of Sound and Vibration* 308 (2007) 268–286.
10. Y. Chen, F. Li, Y. Hao: Analysis of vibration and sound insulation characteristics of functionally graded sandwich plates. *Composite Structures* 249 (2020) 112515.
11. G. Shi: A new simple third-order shear deformation theory of plates. *International Journal of Solids and Structures* 44 (2007) 4399–4417.
12. M. Amabili, S. Farhadi: Shear deformable versus classical theories for nonlinear vibrations of rectangular isotropic and laminated composite plates. *Journal of Sound and Vibration* 320 (2009) 649–667.
13. M. Danesh, A. Ghadami: Sound transmission loss of double-wall piezoelectric plate made of functionally graded materials via third-order shear deformation theory. *Composite Structures* 219 (2019) 17–30.
14. P.R. Saffari, S. Sirimontree, C. Thongchom, T. Jear-siripongkul, P.R. Saffari, S. Keawsawasvong: Effect of uniform and nonuniform temperature distributions on sound transmission loss of double-walled porous functionally graded magneto-electro-elastic sandwich plates with subsonic external flow. *International Journal of Thermofluids* 17 (2023) 100311.

15. A. Muc, J. Flis: Flutter characteristics and free vibrations of rectangular functionally graded porous plates. *Composite Structures* 261 (2021) 113301.
16. M. Vinyas: On frequency response of porous functionally graded magneto-electro-elastic circular and annular plates with different electro-magnetic conditions using HSDT. *Composite Structures* 240 (2020) 112044.
17. V. Gunasekaran, J. Pitchaimani, L.B.M. Chinnapandi: Acoustic radiation and transmission loss of FG-Graphene composite plate under nonuniform edge loading. *European Journal of Mechanics-A/Solids* 88 (2021) 104249.
18. Z. Belabed, M.S.A. Houari, A. Tounsi, S.R. Mahmoud, O.A. Bég: An efficient and simple higher order shear and normal deformation theory for functionally graded material (FGM) plates. *Composites Part B: Engineering* 60 (2014) 274–283.
19. J.L. Mantari, A.S. Oktem, C.G. Soares: Static and dynamic analysis of laminated composite and sandwich plates and shells by using a new higher-order shear deformation theory. *Composite structures* 94 (2011) 37–49.
20. L. Kang, B. Liu, F. An: Beam element resonance-based prediction and parametric analysis of sound transmission of laminated plates. *Applied Acoustics* 199 (2022) 109036.
21. G. Zhang, H. Zheng, X. Zhu: Optimization of composite plates with viscoelastic damping layer for high sound transmission loss under stiffness and strength constraints. *Composite Structures* 306 (2023) 116563.
22. Z. Xu, Z. Zhang, J. Wang, X. Chen, Q. Huang: Acoustic analysis of functionally graded porous graphene reinforced nanocomposite plates based on a simple quasi-3D HSDT. *Thin-Walled Structures* 157 (2020) 107151.
23. A.M.A. Neves, A.J.M. Ferreira, E. Carrera, M. Cinefra, C.M.C. Roque, R.M.N. Jorge, C.M. Soares: Static, free vibration and buckling analysis of isotropic and sandwich functionally graded plates using a quasi-3D higher-order shear deformation theory and a meshless technique. *Composites Part B: Engineering* 44 (2013) 657–674.
24. A.M.A. Neves, A.J.M. Ferreira, E. Carrera, C.M.C. Roque, M. Cinefra, R.M.N. Jorge, C.M.M. Soares: A quasi-3D sinusoidal shear deformation theory for the static and free vibration analysis of functionally graded plates. *Composites Part B: Engineering* 43 (2012) 711–725.
25. A.M.A. Neves, A.J.M. Ferreira, E. Carrera, M. Cinefra, C.M.C. Roque, R.M.N. Jorge, C.M.M. Soares: A quasi-3D hyperbolic shear deformation theory for the static and free vibration analysis of functionally graded plates. *Composite Structures* 94 (2012) 1814–1825.
26. J.G. Berryman: Confirmation of Biot’s theory. *Applied Physics Letters* 37 (1980) 382–384.
27. J.S. Bolton, N.M. Shiau, Y.J. Kang: Sound transmission through multi-panel structures lined with elastic porous materials. *Journal of Sound and Vibration* 191 (1996) 317–347.
28. R. Ye, N. Zhao, D. Yang, J. Cui, O. Gaidai, P. Ren: Bending and free vibration analysis of sandwich plates with functionally graded soft core, using the new refined higher-order analysis model. *Journal of Sandwich Structures & Materials* 23 (2021) 680–710.
29. A. Tian, R. Ye, Y. Chen: A new higher order analysis model for sandwich plates with flexible core. *Journal of Composite Materials* 50 (2016) 949–961.
30. J.N. Reddy: *Mechanics of Laminated Composite Plates and Shells*. CRC Press, 2004.
31. M.R. Zarastvand, M. Ghassabi, R. Talebitooti: A review approach for sound propagation prediction of plate constructions. *Archives of Computational Methods in Engineering* 28 (2021) 2817–2843.

Cite this article as: Zhang Z. Ye R. Ji M. & Zhu G. 2025. A convergence formula for sound transmission loss of composite laminates based on three different shear deformation theories. *Acta Acustica*, 9, 26. <https://doi.org/10.1051/aacus/2025003>.

Appendix A

The nonzero elements in the transfer matrix equation for laminated plates based on CPT are as follows:

$$\begin{aligned}
 S_{11} &= A_{11}\alpha^2 + A_{88}\beta^2, \\
 S_{12} &= (A_{12} + A_{66})\alpha\beta, \\
 S_{12} &= -B_{11}\alpha^3 - (B_{12} + 2B_{66})\alpha\beta^2, \\
 S_{22} &= A_{66}\alpha^2 + A_{22}\beta^2 \\
 S_{23} &= -B_{22}\beta^3 - (B_{12} + 2B_{66})\alpha^2\beta \\
 S_{33} &= D_{11}\alpha^4 + 2(D_{12} + 2D_{66})\alpha^2\beta^2 + D_{22}\beta^4.
 \end{aligned}$$

Appendix B

The nonzero elements in the transfer matrix equation for laminated plates based on FSDT are as follows:

$$\begin{aligned}
 S_{11} &= A_{11}\alpha^2 + A_{66}\beta^2, S_{12} = (A_{12} + A_{66})\alpha\beta, \\
 S_{14} &= B_{11}\alpha^2 + B_{66}\beta^2, \\
 S_{15} &= (B_{12} + B_{66})\alpha\beta, S_{22} = A_{66}\alpha^2 + A_{22}\beta^2, \\
 S_{24} &= S_{15}, S_{25} = B_{66}\alpha^2 + B_{22}\beta^2, \\
 S_{33} &= \kappa(A_{55}\alpha^2 + A_{44}\beta^2), S_{34} = \kappa A_{55}\alpha, \\
 S_{35} &= \kappa A_{44}\beta, S_{44} = D_{11}\alpha^2 + D_{66}\beta^2 + \kappa A_{55}\alpha, \\
 S_{45} &= (D_{12} + D_{66})\alpha\beta, S_{55} = D_{66}\alpha^2 + D_{22}\beta^2 + \kappa A_{44}.
 \end{aligned}$$

Appendix C

The nonzero elements in the transfer matrix equation for laminated plates based on TSDT are as follows:

$$\begin{aligned}
 S_{11} &= A_{11}\alpha^2 + A_{66}\beta^2, S_{12} = (A_{12} + A_{66})\alpha\beta, \\
 S_{13} &= -c_1 \left[E_{11}\alpha^2 + (E_{12} + 2E_{66})\beta^2 \right] \alpha, \\
 S_{14} &= (B_{11} - c_1 E_{11})\alpha^2 + (B_{66} - c_1 E_{66})\beta^2, \\
 S_{15} &= (B_{12} - c_1 E_{12} + B_{66} - c_1 E_{66})\alpha\beta, S_{22} = A_{66}\alpha^2 + 4c_2\beta^2, \\
 S_{23} &= -c_1 \left[E_{22}\beta^2 + (E_{12} + 2E_{66})\alpha^2 \right] \beta, S_{24} = S_{15}, \\
 S_{25} &= (B_{66} - c_1 E_{66})\alpha^2 + (B_{22} - c_1 E_{22})\beta^2, \\
 S_{33} &= \left(A_{55} - 2c_2 D_{55} + c_2^2 F_{55} \right) \alpha^2 + \left(A_{44} - 2c_1 D_{44} + c_1^2 F_{44} \right) \beta^2 + c_1^2 \left[H_{11}\alpha^4 + 2(H_{12} + 2H_{66})\alpha^2\beta^2 + H_{22}\beta^4 \right], \\
 S_{34} &= \left(A_{55} - 2c_2 D_{55} + c_2^2 F_{55} \right) \alpha - c_1 \left\{ (F_{11} - c_1 H_{11})\alpha^3 + (F_{12} - c_1 H_{12}) + 2(F_{66} - c_1 H_{66})\alpha\beta^2 \right\}, \\
 S_{35} &= \left(A_{44} - 2c_2 D_{44} + c_2^2 F_{44} \right) \alpha - c_1 \left[(F_{22} - c_1 H_{22})\beta^3 + [(F_{12} - c_1 H_{12}) + 2(F_{66} - c_1 H_{66})]\alpha^2\beta \right], \\
 S_{44} &= \left(A_{55} - 2c_2 D_{23} + c_2^2 F_{55} \right) + \left(D_{11} - 2c_1 F_{11} + c_1^2 H_{11} \right) \alpha^2 + \left(D_{66} - 2c_1 F_{66} + c_1^2 H_{66} \right) \beta^2, \\
 S_{43} &= \left[\left(D_{12} - 2c_1 F_{12} + c_1^2 H_{12} \right) + \left(D_{66} - 2c_1 F_{66} + c_1^2 H_{66} \right) \right] \alpha\beta, \\
 S_{55} &= \left(A_{44} - 2c_2 D_{44} + c_2^2 F_{44} \right) + \left(D_{66} - 2c_1 F_{66} + c_1^2 H_{66} \right) \alpha^2 + \left(D_{22} - 2c_1 F_{22} + c_1^2 H_{22} \right) \beta^2, \\
 m_{11} &= I_0, m_{22} = I_0, m_{23} = I_0 + c_1^2 I_6 \left(\alpha^2 + \beta^2 \right), m_{34} = -c_1 (I_4 - c_1 I_6) \alpha, m_{35} = -c_1 (I_4 - c_1 I_6) \beta, \\
 m_{44} &= I_2 - 2c_1 I_4 + c_1^2 I_6, m_{55} = I_2 - 2c_1 I_4 + c_1^2 I_6, c_1 = 4 / \left(3h^2 \right), c_2 = 3c_1.
 \end{aligned}$$